Turkish Online Journal of Qualitative Inquiry (TOJQI)
Volume 12, Issue 7, July 2021: 7412 - 7422

Research Article

Classification of Brain MRI Images Based on Segmenting Tumor ROIUsing Histogram Based Multi-Component &Multilevel Adaptive Thresholding

Shrikant Burje[a], Dr. Sourabh Rungta[b], Dr. Anupam Shukla[c]

[a] PhD Scholar, Rungta College of Engineering and Technology, Bhilai, INDIA IIITM Gwalior, M.P, India
[b] Rungta College of Engineering and Technology,Bhilai, INDIA IIITM Gwalior,M.P, India.
[c] Director, IIITM, Pune, Maharashtra, India.

Abstract

The work presented in this paper is focused on extracting the tumor region from Brain MRI images and then classifying them as benign or malignant. The first part comprises detection of tumor part using histogram based multi-component and multilevel adaptive thresholding technique and the later includes tumor and non-tumor part features to classify the MRI images in two classes. The multi-component approach uses all the three components other than the approximation component of wavelet decomposed image for thresholding and the multi-level approach includes two level wavelet decomposition of the original gray level MRI image.The 6-two-dimensional component values at both the levels are transformed and histogram corresponding to each component are down sampled to level 5 using 1D wavelet transform. The Global minimal value at level 5 is the suitably used as a threshold value to filter each individual component and the new image is then reconstructed. Finally, a mean threshold is used to segment the tumor part from the MRI image. The classification using three different classifiers is based on features extracted from the tumor and non-tumor part. Out of 77 normal and 143 affected images, the proposed technique was able to classify the images with greater accuracy.

Keywords: Brain MRI images, benign, malignant, multi-component. multilevel adaptive thresholding, wavelet decomposition, Global minimal value and Neural Network.

1. Introduction

Magnetic Resonance Imaging (MRI) is an effective tool to the surgeons due to its high-quality images of sensitive human organs like brain. The uncontrolled and abnormal cell division creates intracranial mass inside the brain region thus producing brain tumor. These tumors damage and destroy useful cells and or compress other cell within the neighborhood inducing cerebral edema or by exerting internal pressure as they grow and causes inflammation [1].Benign (normal) and malignant (Cancerous) are the primary brain tumors which can be detected and localized or extended. The benign tumors do not spread to other organs and can be removed through surgery. These feared types of cancer cover approximately 2/3 of glioblastoma subjects and affects the sufferer in just 2 years after being diagnosed [2]. The foremost difficulty for the most competent neurochirurgy is to distinguish tumors from the most infiltrating human structure [3]. The survival of childhood tumors to adulthood are subjected to most painful therapies such as Chemotherapy and radiations. Early brain tumor detection solely depends on radiologist experience. The differential diagnostic tool MRI is susceptible to human subjectivity, and a huge magnitude of data id difficult for human analysis [4].

In order to examine whether the tissue is benign or malignant, a biopsy is usually performed. Unlike other organs of the body, a biopsy is not possible and obtained before a brain surgery. For better précised and accurate diagnostics, there is a need to develop an effective diagnostic tool for tumor segmentation and classification from MRI images so that it can bypass surgery and subjectivity [5].Brain tumors segmentation techniques can be segregated in three different approaches: threshold based, region based, clustering based and classification-based methods. The threshold-basedtechnique involves segmenting a region based on a fixed or adaptive value of threshold to segment the ROI from other regions. The approach is to differentiate between ROI intensities and other intensity values. The fixed value thresholding however is limited to the quality of images with respect to homogeneity, illumination variations, noise etc. Region based method starts with a seed point and then either grow or split regions depending on the intensity values of regions. In such cases intensity Homogeneity is the crucial factor. Various similarity measures based on statistical parameters are used to cluster regions corresponding to tumor or other regions. Classification-based methods obtain a set of most effective and discriminating features from MR images. These features help in labelling tumor regions with classification [6].

Overall work is organized as: the existing methodologies related to brain tumor are elaborated in Sect. 2, presented technique is mentioned in Sect. 3, outcomes are highlighted in Sect. 4, and overall work is concluded in Sect. 5.

2. LITERATURE REVIEW

Most of the recent work proposed in the literature is based on segmenting the tumor part and then extracting statistical and textural features to classify the MRI images. The researchers have used either textural, statistical or hybrid features for classification, while the classifiers mainly include SVM, Fuzzy and CNN. This part of the paper introduces some of the recent contributions by the researchers in the field of brain tumor detection and classification. Milica M. Badza and Marko C. Barjaktarovic [7] used a simpler CNN to classify MRI images using two 10 cross fold validation and over two datasets thus developing effective decision-support tool for radiologists in medical diagnostics. The network was tested over n T1-weighted contrast-enhanced magnetic resonance images and with good generalized network along with execution speed obtained 96.56% classification accuracy.

A two-phase model for fast brain tumor segmentation with training phase for computing weights for optimized U-Net and an adaptive threshold value and testing phase for a trained U-Net model predicting a rough tumour segment is proposed in [8]. The model was worked out for 3064 images and outperforms other techniques in terms of recall and dice similarity, training time and precision and accuracy compared to Resnet34.An automatic segmentation method overcoming tumor shape, size, location, and overlapping with other tissue based on convolutional neural networks (CNN) was presented in [9] over two different datasets. To prevent possible overfitting in the training phase, weights of a pre-trained network were used as initial weights of neurons and overlapping difficulties were overcome using morphological operations in the pre-processing stage. A hybrid CNN model was designed by removing the last 5 layers of the Resnet50 model and adding 8 new layers for brain tumor detection in [10]. The accuracy noted was 97.2% over Kaggle dataset having 253 MRI images. The work presented in [11] distinguished between normal and abnormal pixels, using 5-layer CNN, based on texture based and statistical based features where Fuzzy C-Means clustering algorithm was employed to extract the tumor region. Compared to other traditional classifier, CNN was able to classify tumor and non tumor pixels in BRATS dataset images with an accuracy of 97.87%.An empirical approach to explore new areas to find the appropriate class distribution for the training set in different problems using CNN was introduced in [12]. The authors suggested patch-wise CNN classifier to automate brain tumor segmentation and focused on optimizing through variations in input patch size. They concluded that increasing the patch size to 33x33 enhances the segmentation accuracies of all tumor regions, but increasing the patch size beyond 33×33 resulted in lower accuracies in segmenting the fluid surrounding the tumor (edema).

A combination of k-means clustering, patch-based image processing, object counting, and tumor evaluation was found to be capable of detecting multiple tumours in MRI images regardless of their intensity level variations, size, and location including those with very small sizes [13]. The average values for Precision, Accuracy, and Specificity were found to be 98.48, 99.81, and 99.99% respectively. The Dice Score Coefficient

average value was 95.81%, while the Recall average value was 92.16%.Muhammad Sharif et. al. [14] used triangular fuzzy median filtering for image enhancement and unsupervised fuzzy sets for tumor segmentation. Similar texture features based on Gabor features were extracted from BRATS 2012, 2013, 2014 and 2015 and 2013 Leader board for tumor classification using extreme machine learning and regression ELM. Their method provided accurate and efficient segmentation and classification with average computational time of 0.7136s.

An automated method is proposed to easily differentiate between cancerous and non-cancerous MRI of the brain using Support Vector Machine (SVM) with variations in cross validation on same set of features [15]. The features were extracted based on shape, texture, and intensity of the MRI images. The method achieved average 97.1% accuracy, 0.98 area under curve, 91.9% sensitivity and 98.0% specificity with low computational time. The work proposed in [16] uses axial and Coronal slice of single-spectral structural 2D MRI images which are spliced into two halves (two hemispheres left and right) to reduce the computational time and statistical features are then extracted for classification using SVM. The average accuracy was found to be 92.5% with less execution time as compared to others on BRATs database.

3. PROPOSED METHODOLOGY

The system block diagram is shown in figure 1 which shows basically two stages: Segmentation and Feature Extraction. The first part deals with segmentation of tumor region and the second part includes classification using three classifiers based on extracted features.

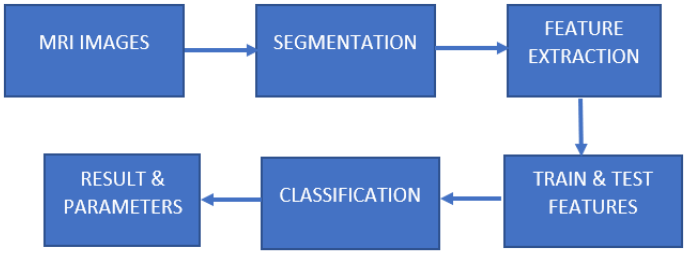

Figure 1 – General block diagram of the proposed work

The process of extraction of feature vector element for both the training and test set is equivalent and follows the steps mentioned below in the figure 1. The system uses 143 affected and 77 normal Brain images form the KAGGLE dataset for Brain tumor segmentation and classification. The dataset consists of four class brain images corresponding to Glioma_tumor, Meningioma_tumor, Pituitary_tumor and No_tumor with two independent folders for training and testing. The following table 1 shows the characteristics of the dataset.

Table 1 – KAGGLE dataset description for number of images

Sr. No.	Class	No. of images for Training	No. of images for Testing
1	Glioma_tumor	826	100
2	Meningioma_tumor	822	115
3	Pituitary_tumor	827	74
4	No_tumor	395	105

We have considered the problem for two classes: Normal (No_tumor class) and Affected (Glioma_tumor, Meningioma_tumorand Pituitary_tumor). The main aim of the work was to focus on segmenting the tumor region to the near accurate and after extracting the affected part, features in this region of interest were then used for training the classifier for classification. Therefore, the three classes Glioma_tumor, Meningioma_tumor and Pituitary_tumor was considered in a single class. The KAGGLE Dataset class images show variations with respect to posture of the head region, illuminations and edges of the brain structures. We have selected only

those images where the background (Non affected region) is darker compared to the affected region (The tumor part). Also, the flattened section images were considered neglecting skull and side view images. Some of the type of images not considered in this work are shown below in figure whereas some of the valid images for this work are shown in figure 2 and 3. Figure 4 & 5 shows images from normal and affected dataset considered in this work where the brain region and the tumor region show proper illumination. Images in which there is slight variation between tumor part and the non-affected brain part are not considered since the system will provide poor segmentation thus resulting in misclassification.

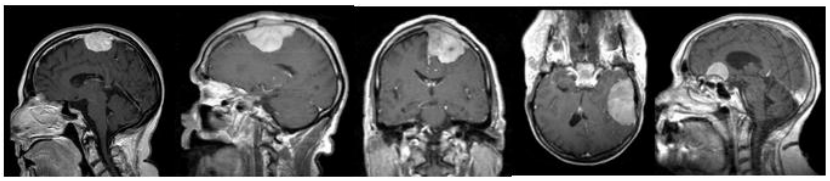

Figure 2 – Affected Skull and Side View images

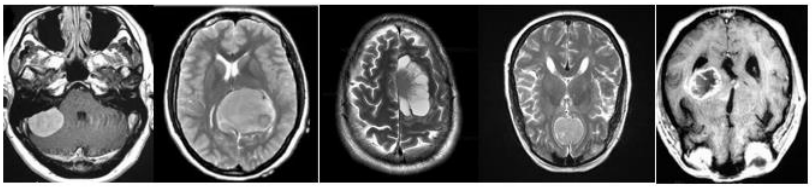

Figure 3 – Affected frontal images with improper illuminations

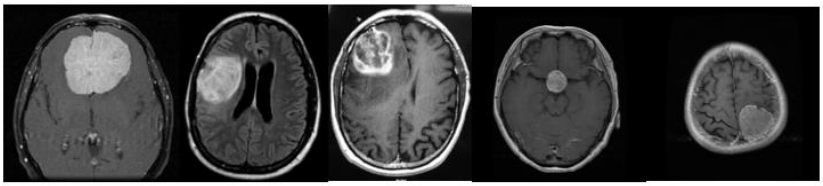

Figure 4 – Some valid affected frontal images for the system

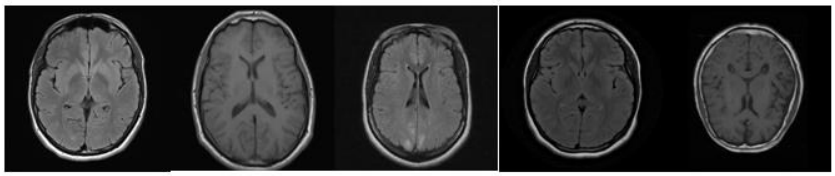

Figure 5 – Some valid normal frontal images for the system

A. Segmentation

This part deals in locating the tumor region in the brain MRI images. The main problem in locating the actual tumor part is the presence of hard tissues either inside the brain region or at the outer edges of the brain where the intensities of these hard tissues match with the tumor region. Therefore, the system proposed in this paper apply two stage segmentation process where the background pixels are eliminated first and then the elimination of other hard tissues is done.The miscellaneous tissues are subjected to a threshold which depends on the window size of the filter being applied over the segmented part from the first stage. The first stage segmentation solely depends on adaptive threshold analytically calculated over the Histogram of the Original gray scale image which is decomposed using 2D and 1D Wavelet Transformsuccessively. The Original image is decomposed up to level 2 using mother wavelet Debauchees 6 transform to generate 8 components as indicated in figure 6 and 7. Three components at both levels including horizontal, vertical and diagonal are filtered out

using individual adaptive threshold for each component. The individual threshold for each component is the valley point (global minima) obtained from the 1D level 5 Detail component of the histogram of each of the decomposed wavelet component and mapped in the range [0 255] of the original histogram of the 2D component.

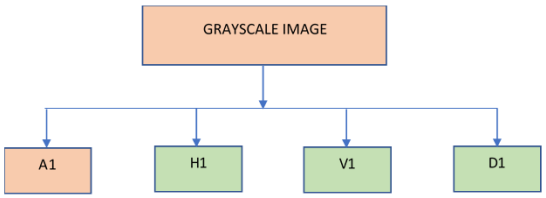

Figure 6 – 2D wavelet transform at level 1. A1, H1, V1 and D1 representing the Approximation, Horizontal, Vertical and Detail components.

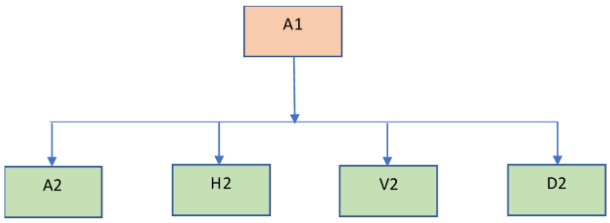

Figure 7 – 2D wavelet transform at level 2.

It is clear that wavelet coefficients are real numbers and the range of values depends on the pixel intensities in the MRI images. Obviously, for histogram, these real values need transformation from the current range to [0 255] range. The transformation functions used is listed below:

1. Find the minimum value in the wavelet component after decomposition.
2. If the minimum value is negative, add the absolute value of minimum value to all numbers in the component, otherwise subtract it. This will make the minimum value to zero.
3. Find the maximum value.
4. Divide all values in the component by this maximum value. This will yield a maximum value of 1.
5. Multiply all values by 255. This will make the maximum value to be 255.
6. Round all values and store them as 8-bit unsigned integer.

After the histogram is obtained for all 6 components excluding the approximation components (One of the histograms for level 1 detail component is shown in figure 8(a)), these histograms are further decomposed to level 5 using 1D wavelet transform (The plot at level 5 using 1D decomposition is shown in figure 8(b)). No matter, shifting the values would cause error and the thresholds so obtained may not be accurate enough to filter out the components correctly. The same error can be worked out by GLOBAL thresholding, which is used after the image is reconstructed.

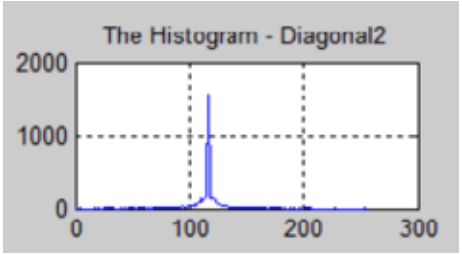

(a)

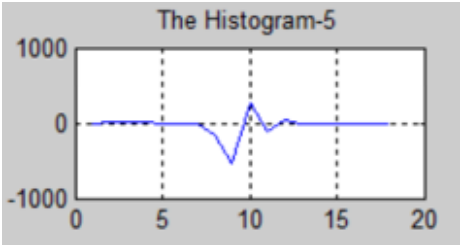

(b)

Figure 8 – (a) Histogram of 2nd level 1D wavelet decomposition for Detail component and (b) detail coefficients plot at level 5 decomposition.

The figure 8(b) indicates a Global Minima for the detail component for level 2 at thd2=8 for say n=18 samples. This Global Minima is the threshold to filter the component at level 5. To map this threshold for N=256 samples in figure 8(a), the following mapping is carried out, where x represents the general term for the index1 and 2 levels.

$$THDx = \frac{thdx * N}{n} \qquad [1]$$

Similarly, all the 6 thresholds THD1, THV1, THD1, THD2, THV2 and THD2 are evaluated and their corresponding component values are filtered. If the coefficient value is less than the threshold, it is made zero, otherwise the coefficient value is kept as it is.Finally, the filtered components are combined with their respective approximation components and the reconstructed imagesare obtained at both levels. Figure 9 illustrate the effect of reconstructions at both levels. The error introduced by shifting the values using transformation is now diluted by finding another GLOBAL threshold which is the mean of all the individual component thresholds calculated above. The global threshold is given by the following equation and y represents alphabets H,V and D for three components.

$$THG = \sum_{m=1}^{6} THyx \qquad [2]$$

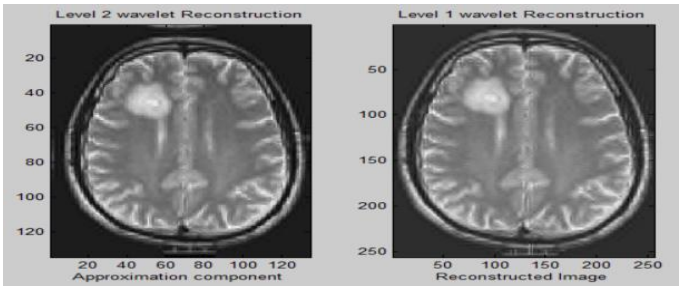

Figure 9 – Reconstructed Approximation component from level 2 and final reconstruction.

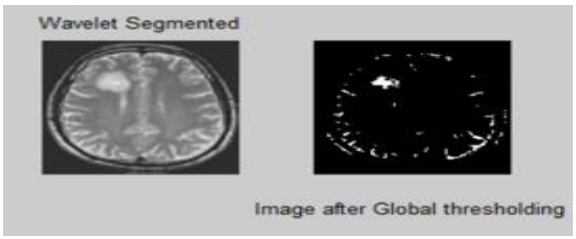

Figure 10- Wavelet-based segmentation and image obtained after the application of Global threshold.

It is seen from figure 10 that the output obtained after global thresholding eliminates background pixels and only the tumor region along other small regions conforming the hard tissues are left out. In case when the hard tissues cover a small portion of the entire brain image, the output image seems to be noisy with clear tumor region and low-density hard tissue pixels. In some cases, when the brain region is homogeneous, the tumor is

only the part which exists after global thresholding and there is no need for further processing. But the Kaggle dataset have few numbers of images which satisfy the last condition. Therefore, a post filtering operation is performed to eliminate the false pixels which are similar to tumor pixels but actually they do not contribute to the tumor region as such.

The post processing step involves filtering the false pixels by assuming a window of size win=15x15 and eliminating those pixels who satisfies the condition below:

Check the Neighborhood around suspicious pixel (value 1), if the neighborhood sum is less than Threshold, change the pixel to background, otherwise define it to suspicious area. Let x be the suspicious pixel (intensity value 1) after global thresholding, 'psum' is the sum of all pixel values in the neighborhood (15x15 with center as x) of x and winsize=15*15, then,

$$f(x) = \begin{cases} 0, & psum < winsize/2 \\ x, & psum \geq winsum/2 \end{cases} \qquad [3]$$

The size of the window is determined experimentally by subjecting most of the images to the system from the dataset. A low size window will not be able to filter out the false pixels and leave out dots of hard tissues over the hard edges, whereas a larger window will not only remove the hard tissues but also eliminate the suspicious pixel. The result of the last stage filtering is shown below in the figure 11.

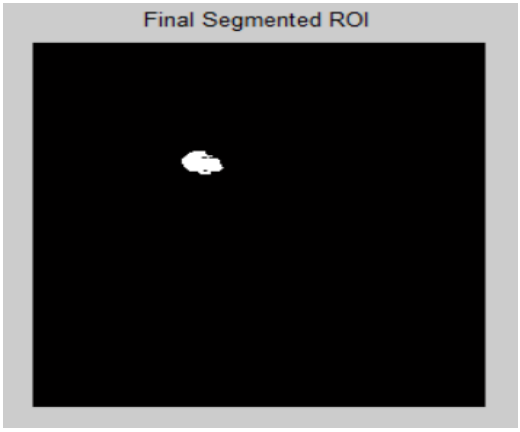

Figure 11 – The final segmented image

B. Feature Extraction

Once the final segmented image is obtained, the class (either 0 for normal or 1 for affected) is found just by summing the suspicious pixels in the resultant image. Experimentally we conducted tests over all 220 images and found that if the count of suspicious pixels is above S=10, the tumor exists and if it is below or equal to 10, the brain image belongs to normal of no-tumor category. We have extracted the region of original gray scale image considering mask of the final segmented ROI as shown in figure 12(a) to extract features in the affected images. Whereas when a normal gray scale image is segmented, no such mask is obtained due to absence of the tumor region. In such case, a center mask with a square region in the middle of [56 56] pixel is considered for feature extraction from the original gray scale image shown in figure 12(b). This will consider the intensity pixels of the tumor region in the affected images and non-tumor part in the normal images with some hard tissue artifact in few images. This will result in a feature image. Rest of the region excluding the concentrated part in both of the affected and normal images was made zero or black. To extract the features, a 2D wavelet transform was carried out on the feature images to level 5. The approximation component is then converted to row vector and again decomposed to level 4 using 1D wavelet transform resulting in a 30 element (coefficient) vector as

input to the classifiers indicated by figure 12(c). Thus, the input vector matrix for normal images and affected images are 30x77 and 30x143 (one affected image neglected) respectively.

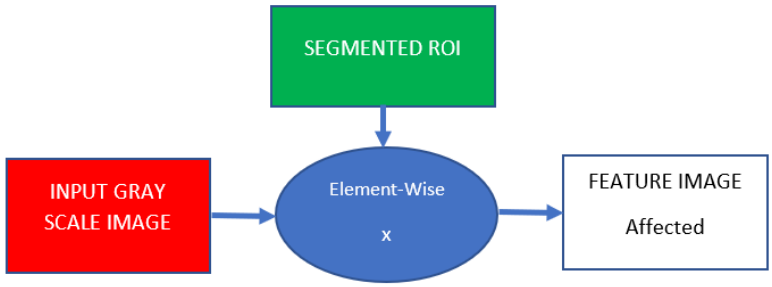

(a)

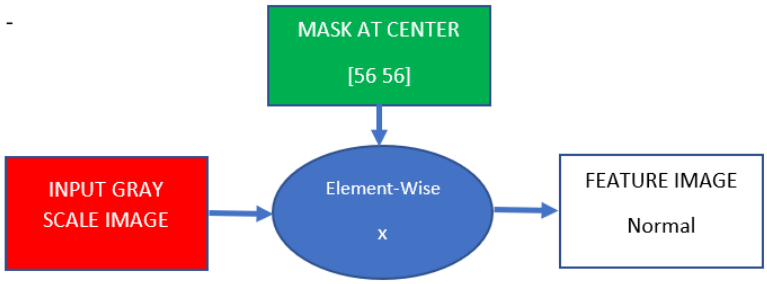

(b)

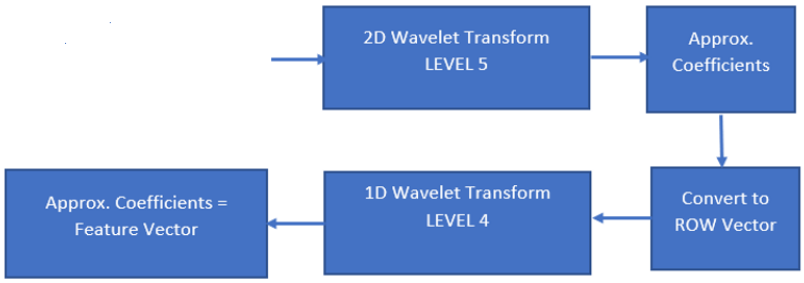

(c)

Figure 12– Block diagram showing feature extraction process (c). (a) and (b) indicates the construction of feature images for affected and normal images

C. The Classifiers

The Radial Basis network consists of three layers including strictly one hidden layer with input and the output layer. It transforms the input to other form which is then feed to the network to achieve linear separability. Nodes in the hidden layer perform the radial basis transformation and the output layer performs the linear combinations of the hidden layer output to result in probabilistic value output. The radial basis function and the output of the network is given by equations 4 and 5.

$$h(x) = \exp\left[-\frac{(x-c)^2}{r*r}\right] \qquad [4]$$

$$f(x) = \sum_{j=1}^{m} w_j * h_j(x) \qquad [5]$$

radial distance r = ||x- t||; t being the receptor

The RBF network was used with the default parameters having spread=1, Goal=0.0 and Q=Number of inputs (Maximum number of neurons in the hidden layer).

Feed Forward Networks are the common types of Neural Networks used in large applications which uses Backpropagation training algorithms. Due to the fact that it needs proper tunning of parameters these networks are replaced by other non-linear problem-solving networks nowadays where few parameters are required to be tunned during initialization. For a comparative approach we have used Feed Forward Networks with the following specifications listed in table 2.

Table 2 – Initialized parameters for FFNN

Sr. No.	Parameter	Value
1	Number of Hidden Layers	3
2	Neurons	[60 30 1]
3	Transfer Functions	{'logsig','logsig','purelin'}
4	Epoch	500
5	Goal	1e-6
6	Minimum Gradient	1e-20
7	Learning Rate	0.1
8	Performance Factor	MSE

Support Vector Machine (SVM) also known as discriminative classifier is the most popular and widely used classifier with supervised learning and offers high accuracy as compared to other networks. It is known for its kernel trick to handle nonlinear input spaces. SVM separates samples using a Hyperplane with larger space margin. It is capable of finding the optimum boundary for new set of inputs. The SVM kernel (linear, polynomial and Radial Basis Function) transform the low dimensional input space (Non-separable) to high dimensional space(Separable).

4. RESULTS & CONCLUSIONS

The result of segmentation is indicated in figures 13(a) to (e) below where the affected part is shown by white intensity pixels. The segmented part looks smaller as compared to shown in original gray scale image due to the fact that the reconstructed image using wavelet transform have lower dimension [249 249].

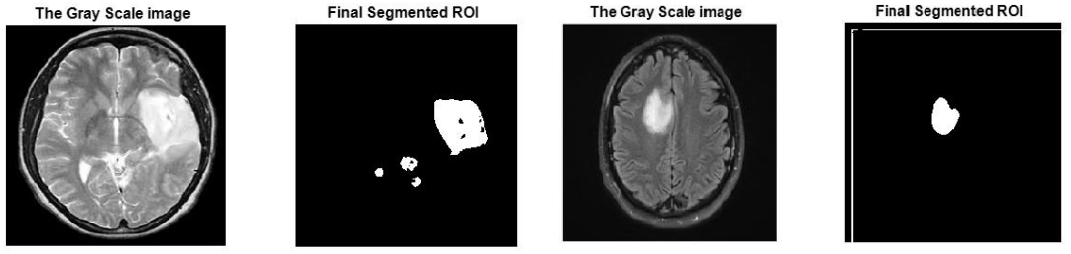

(a) (b)

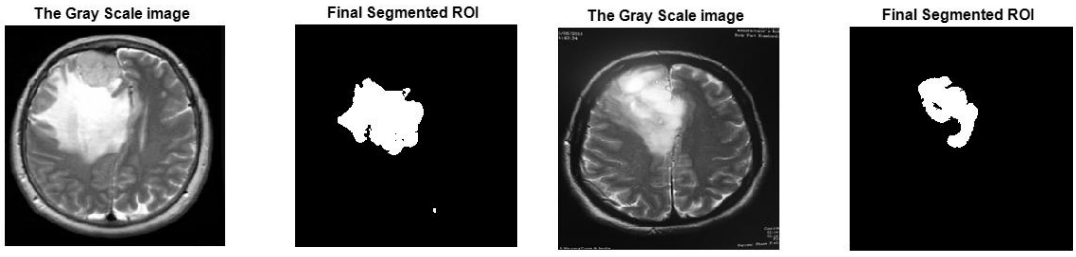

(c) (d)

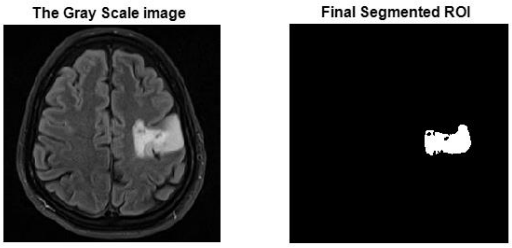

(e)

Figure 13 – (a) to (e) indicates the result obtained after segmentation for gray scale MRI images.

A 7 cross fold validation and a 10 cross fold validation was used for better performance for normal and affected features. That is at any instant, 66 samples each of 30 inputs was used for training and 11 samples with 30 inputs were used for testing the classifiers for normal images. Similarly, 110 samples were used for training and 33 samples were used for testing the classifier for affected images. Again, for each batch in normal features, all batches of affected features were considered resulting in 70 combinations to a classifier to evaluate the performance for the test samples of size 11+33=44. The table 3 given below indicates the performance of all the three classifiers viz. RBFNN, SVM and FFNN. The first 11 samples(marked with RED color) belong to normal images where the expected output for all 70 combinations is 0 and remaining 33 (marked with BLUE color) belong to affected images where the expected output for all 70 combinations is 70 since the target values for normal and affected images are 0 and 1 respectively. A threshold of 0.5 had been used to the output obtained after simulating the networks for RBFNN and FFNN. The output obtained in the table shows that RBFNN performed better for normal images while SVM performed better for affected images (BOLD Marked). The FFNN performed better in 2 samples exclusively. It can be seen that a THRESHOLD=15 will differentiate normal samples from the affected ones for all the classifiers.The values in first 11 rows should be 0 for normal images. A higher value indicated misclassification out of 70 combinations, whereas a lower value than 70 in remaining rows from 12 to 44 indicates misclassification for affected images with magnitude (70-value). For example, values in row 1 states that RBF classified correctly while there were 10 and 8 misclassifications in 70 combinations for SVM and FFNN.

Table 3 – Performance of RBFNN, SVM and FFNN for 44 test samples (11 normal and 33 affected) considering sum of 70 different combinations.

Sample	RBF	SVM	FFNN	Sample	RBF	SVM	FFNN	Sample	RBF	SVM	FFNN
1	**0**	10	8	16	57	**66**	64	31	52	**70**	60
2	**0**	**0**	2	17	65	**65**	64	32	68	**70**	69
3	**0**	**0**	2	18	61	**65**	64	33	64	64	**66**
4	**0**	**0**	3	19	47	**70**	64	34	56	**70**	63
5	**0**	**0**	3	20	56	**70**	62	35	56	**65**	64
6	**0**	10	8	21	63	**70**	66	36	58	**70**	70
7	4	**0**	5	22	**64**	**64**	63	37	63	**70**	70
8	**0**	10	11	23	65	**70**	65	38	48	**67**	62
9	**0**	**0**	4	24	48	**64**	62	39	61	64	**65**
10	1	**0**	3	25	54	**70**	**70**	40	60	**64**	63
11	**0**	**0**	4	26	61	**70**	**70**	41	56	**70**	64
12	51	**70**	62	27	54	**63**	58	42	52	**70**	68
13	47	**65**	61	28	**65**	**65**	61	43	69	**70**	66
14	58	**70**	69	29	59	**65**	**65**	44	64	**65**	64
15	62	**70**	69	30	55	**70**	60				

The proposed technique adopting adaptive thresholding was able to segment the region of interest and classify the images accurately. Experimentally, it was found that the window size affects locating the tumors with larger window size missing low-density tumors and lower window size covering the hard tissue as a tumor part. Also, we had considered minimum 10 pixels for a tumor region which means the algorithm will not be able to detect tumors of size less than 10 pixels. More robust features can be obtained to improve the performance of the system before the classification. We used the tumor region and the brain region for extracting the features in affected and normal images wherein a large portion was set to black thus with no contributions in the feature vector. All other MRI images from the dataset can be considered designing a more robust system which can handle illumination variations and edge characteristics.

REFERENCES

[1] "The essential guide to brain tumors", National brain tumor society (NBTS), 2007.

[2] Waseem Khan," Image Segmentation Techniques: A Survey", Journal of Image and Graphics Vol. 1, No. 4, December 2013 4.

[3] Prateek Kumar Garg et al.," A Survey Paper on Various Median Filtering Techniques for Noise Removal from Digital Images", American International Journal of Research in Formal, Applied & Natural Sciences, 7(1), June-August, 2014.

[4] Afshar P., Plataniotis K.N. and Mohammadi A., "Capsule Networks for Brain Tumor Classification Based on MRI Images and Coarse Tumor Boundaries", In Proceedings of the ICASSP 2019–2019 IEEE International Conference on Acoustics, Speech and Signal Processing (ICASSP), Brighton, UK, 12–17 May 2019; pp. 1368–1372.

[5] Byrne J., Dwivedi R. and Minks D., "Tumours of the brain. In Nicholson T (ed) Recommendations Cross Sectional Imaging Cancer Management", 2nd ed., Royal College of Radiologists: London, UK, 2014; pp. 1–20. Available online: https://www.rcr.ac.uk/publication/recommendations-cross-sectional-imaging-cancer-managementsecond-edition (accessed on 5 November 2019).

[6] Bala Venkateswarlu Isunuri & Jagadeesh Kakarla, "Fast brain tumour segmentation using optimized U-Net and adaptive thresholding", Journal for Control, Measurement, Electronics, Computing and Communications, Automatika, VOL. 61, NO. 3, 352–360, 2020.

[7] Milica M. Badza and Marko C. Barjaktarovic, "Classification of Brain Tumors from MRI Images Using a Convolutional Neural Network", Appl. Sci., 10, 1999, 2020.

[8] Bala Venkateswarlu Isunuri & Jagadeesh Kakarla, "Fast brain tumour segmentation using optimized U-Net and adaptive thresholding", Journal for Control, Measurement, Electronics, Computing and Communications, Automatika, VOL. 61, NO. 3, 352–360, 2020.

[9] [9] Neural Network Architecture for Brain Tumor Segmentation in 3D Brain Magnetic Resonance Imaging", Multidisciplinary Cancer Investigation, Volume 4, Issue 1, January 2020.

[10] Ahmet Çinar and Muhammed Yildirim, "Detection of tumors on brain MRI images using the hybrid convolutional neural network architecture", Medical Hypotheses, 139, 109684. 2020.

[11] Tonmoy Hossain et. al., "Brain Tumor Detection Using Convolutional Neural Network", 1st International Conference on Advances in Science, Engineering and Robotics Technology 2019 (ICASERT 2019), IEEE, 2019.

[12] Mohamed Babikir Ali, Ruba Ali Hamad and Mohanned Ahmed, "Optimizing Convolutional Neural Networks for Brain Tumor Segmentation in MRI Images", International Conference on Computer, Control, Electrical, and Electronics Engineering (ICCCEEE), IEEE 2018.

[13] Mohamed Nasor and Walid Obaid, "Detection and Localization of Early-Stage Multiple Brain Tumors Using a Hybrid Technique of Patch-Based Processing, k-means Clustering and Object Counting", International Journal of Biomedical Imaging, Volume 2020.

[14] Muhammad Sharif et. al., "Brain tumor detection based on extreme learning", Neural Computing and Applications, Springer, January 2020. https://doi.org/10.1007/s00521-019-04679-8.

[15] Javeria Amin et. al., "A distinctive approach in brain tumor detection and classification using MRI", Pattern Recognition Letters, 1-10, 2017.

[16] Pratima Purushottam Gumaste and Vinayak K. Bairagi, "A Hybrid Method for Brain Tumor Detection using Advanced Textural Feature Extraction", Biomedical & Pharmacology Journal, Vol. 13(1), p. 145-157, 2020.